INSTITUTE OF PHYSICS PUBLISHING INVERSE PROBLEMS

Inverse Problems **17** (2001) 1203–1218 www.iop.org/Journals/ip PII: S0266-5611(01)17835-4

Inverse homogenization for evaluation of effective properties of a mixture

Elena Cherkaev

University of Utah, Department of Mathematics, 155 South 1400 East, JWB 233 Salt Lake City, UT, 84112, USA

E-mail: elena@math.utah.edu

Received 6 October 2000, in final form 7 June 2001

Abstract

The paper deals with indirect evaluation of the effective thermal or hydraulic conductivity of a random mixture of two different materials from the known effective complex permittivity of the same mixture. The method is based on deriving information about the microstructure of the composite from measurements of its effective properties; we call this approach inverse homogenization. This structural information is contained in the spectral measure in the Stieltjes representation of the effective complex permittivity. The spectral measure can be reconstructed from effective measurements and used to estimate other effective properties of the same material. We introduce S-equivalence of the geometric structures corresponding to the same spectral measure, and show that the microstructures of different mixtures can be distinguished by the homogenized measurements up to the introduced equivalence. We show that the identification problem for the spectral function has a unique solution, however, the problem is extremely ill-posed. Several stabilization techniques are discussed such as quadratically constrained minimization and reconstruction in the class of functions of bounded variation. The approach is applicable to porous media, biological materials, artificial composites and other heterogeneous materials in which the scale of microstructure is much smaller than the wavelength of the electromagnetic signal.

1. Introduction

This paper deals with heterogeneous materials in which the scale of inhomogeneity is much smaller than the wavelength of the electromagnetic signal. Examples of such media are numerous: sea ice with a random structure of brine and ice, fluid-filled lungs, porous bones or oil-bearing rocks and artificial composites. In these materials, fine scale variations of the random microstructure cannot be resolved by the effective electromagnetic measurements. Only information about the averaged or homogenized structure is present in the measurements of the effective complex permittivity. On the other hand, the different effective properties of the same mixture are related through its geometry. This phenomenon is a basis for widely used empirical and semi-empirical relations, such as for instance, Kozeny–Carman or Katz–Tompson relations providing an estimate for permeability of a porous material. Geometric characterization of the medium is often introduced through the 'formation factor' F which relates the properties of one phase in the mixture to the effective properties of the material: $F = \sigma/\sigma^*$, where σ is the conductivity of a fluid filling in the porous material, and σ^* is the effective conductivity.

In principle, the geometric structure of a fine scale random material can be reconstructed using direct methods such as, for example, x-ray computed tomography. The reconstructed geometry can be characterized by the correlation functions; using them some properties of the medium can be evaluated [9, 16]; these are the volume fractions of the materials, specific surface area, or fractal dimension. Computation of the effective properties of such a complicated finely scaled medium is a large computational problem. This paper uses an indirect method of characterizing the geometric structure of the mixture. The method is based on deriving information about a geometric 'structural function' of the composite from its effective properties; we call this approach *inverse homogenization* [15].

Accounting for the geometry of the composite was exploited starting from the pioneering work of Prager [32], in deriving coupled bounds on the effective material properties. Coupled or cross-property bounds use measurements of one effective property to improve bounds on other effective properties. The work of Prager who used bounds on the effective magnetic permeability μ^* to improve bounds on the thermal conductivity γ^* and on the permeability of the same material at other temperatures, was followed by a number of papers by different authors.

This paper proposes to measure the effective response of the random medium for a range of different parameters of the applied fields; we demonstrate that the geometric structural function of the mixture can be reconstructed from such data. The geometric structural function is associated with the spectral measure μ in the Stieltjes integral representation of the effective property of the mixture. This analytic representation of the effective complex permittivity ϵ^* was developed by Bergman [4, 5], Milton [29], and Golden and Papanicolaou [23] in the course of computing bounds for the effective permittivity of an arbitrary two component mixture. The spectral function μ was used to derive microstructural information about the composite [15, 21, 27, 28], to appraise the accuracy of the permittivity measurements [20], and to model the effective complex conductivity of geological mixtures [14, 24, 36] or of random resistor networks [17]. This function was calculated from reflectivity measurements in [18].

Here we show that the spectral function μ in the Stieltjes integral representation can be uniquely reconstructed if the effective property of the mixture is known on an open set, say on an arc in a complex plane. This is the case when measurements of the effective complex permittivity ϵ^* are available in an interval of frequency of applied electromagnetic field, provided that the properties of the constituents are frequency dependent. The spectral measure is determined by the structure of the mixture, it is the same for different effective properties. Having reconstructed this function from one set of data, we can use it to compute other effective properties such as thermal or hydraulic conductivity of the same mixture.

From the computational point of view, the problem of reconstruction of the spectral measure μ is extremely ill-posed: it is equivalent to the inverse potential problem, in particular, to the inverse problem of gravitational potential. This problem has many applications in geophysics and is well studied in mathematical as well as geophysical literature (see, for instance, monographs on the inverse source problem [2, 25] and on the geophysical inverse problem [31]).

To obtain a stable reconstruction of the spectral measure, we develop a regularization approach based on constrained least squares minimization. Constraint in a form of the l^2-norm of the solution gives oversmoothed reconstruction. Total variation of the solution introduced as a constraint leads to reconstruction in a class of functions of bounded variation. Since the function μ is indeed a function of bounded variation, total variation penalization seems to be an appropriate technique. We should also note that computation of the effective thermal conductivity or other effective properties involves a smoothing operator, which relaxes the influence of noise in the data. Hence, in spite of severe ill-posedness of the measure reconstruction, the final result is reasonably stable.

2. Problem of estimation of different effective properties of a random mixture

We consider a stationary random medium, occupying a region $\mathcal{O}$ in $\mathbb{R}^d$, where $d = 2$ or $d = 3$. The medium is a fine scale mixture of two materials with the values of the complex permittivity ϵ_j and the thermal conductivity γ_j in a region $\mathcal{O}_j$, $j = 1, 2$, with $\mathcal{O} = \mathcal{O}_1 \cup \mathcal{O}_2$. We assume that the characteristic size of the inhomogeneities is microscopical in comparison with the size of the region $\mathcal{O}$, and introduce the characteristic function χ of the region $\mathcal{O}_1$ occupied by the first material for a realization $\eta \in \Omega$, where Ω is the set of all realizations of the random medium:

$$\chi(x, \eta) = \begin{cases} 1, & x \in \mathcal{O}_1, \\ 0, & \text{otherwise.} \end{cases} \tag{1}$$

The characteristic function of the domain occupied by the second material is $1 - \chi(x, \eta)$. Suppose that two different fields are applied in this random medium, the electric field, E_ϵ, and the temperature gradient field, E_γ. The complex permittivity of the medium is modelled by a (spatially) stationary random field $\epsilon(x, \eta)$, $x \in \mathbb{R}^d$ and $\eta \in \Omega$, $\epsilon(x, \eta) = \epsilon_1 \chi(x, \eta) + \epsilon_2(1 - \chi(x, \eta))$. Similarly, the thermal conductivity is $\gamma(x, \eta) = \gamma_1 \chi(x, \eta) + \gamma_2(1 - \chi(x, \eta))$. Since the stationary fields are described by similar equations, we can introduce the notation σ equal to ϵ to denote an electric field, and equal to γ to denote a temperature gradient field. The stationary random fields $E_\sigma(x, \eta)$ and $J_\sigma(x, \eta)$ are related by $J_\sigma(x, \eta) = \sigma(x, \eta) E_\sigma(x, \eta)$ and satisfy the equations

$$\nabla \cdot J_\sigma = 0, \qquad \nabla \times E_\sigma = 0, \qquad \langle E_\sigma(x, \eta) \rangle = e_k, \qquad \sigma = \epsilon, \gamma. \tag{2}$$

Here e_k is a unit vector in the kth direction, for some $k = 1, \ldots, d$, and $\langle \cdot \rangle$ means ensemble average over Ω or spatial average over all of $\mathbb{R}^d$. The effective tensor $\boldsymbol{\sigma}^*$ is defined as a coefficient of proportionality between the averaged fields: $\langle J_\sigma \rangle = \boldsymbol{\sigma}^* \langle E_\sigma \rangle$. Hence the effective property tensors $\boldsymbol{\epsilon}^*$ and $\boldsymbol{\gamma}^*$ are $\langle J_\epsilon \rangle = \boldsymbol{\epsilon}^* \langle E_\epsilon \rangle$ and $\langle J_\gamma \rangle = \boldsymbol{\gamma}^* \langle E_\gamma \rangle$.

We notice that both problems are related by the same function χ:

$$\nabla \cdot (\epsilon_1 \chi(x, \eta) + \epsilon_2(1 - \chi(x, \eta)))\, E_\epsilon = 0, \qquad \boldsymbol{\epsilon}^* = \langle \epsilon E_\epsilon \rangle \tag{3}$$

and

$$\nabla \cdot (\gamma_1 \chi(x, \eta) + \gamma_2(1 - \chi(x, \eta)))\, E_\gamma = 0 \qquad \gamma^* = \langle \gamma E_\gamma \rangle. \tag{4}$$

Suppose that one of the effective properties, ϵ^* (see (3)), can be measured. The problem is to find the other effective property γ^* using (4).

We consider here isotropic mixtures and focus on one diagonal coefficient $\epsilon^* = \epsilon^*_{kk}$ and $\gamma^* = \gamma^*_{kk}$. Due to homogeneity of effective parameters, $\epsilon^*(c\epsilon_1, c\epsilon_2) = c\epsilon^*(\epsilon_1, \epsilon_2)$ for any constant c, ϵ^* depends only on the ratio $h = \epsilon_1/\epsilon_2$. Let $m(h) = \epsilon^*(h)/\epsilon_2$. The function $m(h)$ is analytic off $(-\infty, 0]$ in the h-plane, and it maps the upper half plane to the upper half plane [4, 23]. Hence $m(h)$ is a Herglotz function [3]. We recall that a Herglotz function $\phi(\zeta)$, $\zeta \in \mathbb{C}$, is analytic for $\operatorname{Im}\zeta \neq 0$, and such that $\operatorname{Im}\phi(\zeta)$ and $\operatorname{Im}\zeta$ have the same sign for all ζ. Such a function admits the integral representation (see [3, p 262]),

$$\phi(\zeta) = \alpha\zeta + \beta + \int_{-\infty}^{\infty} \frac{\zeta u + 1}{u - \zeta}\, \mathrm{d}\nu\,(u) \tag{5}$$

with a bounded and nondecreasing function $\nu(u)$ on $-\infty < u < \infty$. Here β is real, and $\alpha \geqslant 0$. Provided the first moment of ν is finite, this representation can be brought to the following form:

$$\phi(\zeta) = \alpha\zeta + \beta' \int_{-\infty}^{\infty} \frac{\mathrm{d}\mu\,(u)}{u - \zeta}, \tag{6}$$

where

$$\mathrm{d}\mu\,(u) = (1 + u^2)\, \mathrm{d}\nu\,(u), \qquad \text{and} \qquad \beta' = \beta - \int_{-\infty}^{\infty} u\, \mathrm{d}\nu\,(u). \tag{7}$$

Based on this approach, a representation for ϵ^* was developed in [4] for periodic composites (see also [7, 30]). A general integral representation for ϵ^* with a positive Borel measure μ on [0, 1] was obtained in [23], and can be formulated as follows. Introduce a function $F(s)$:

$$F(s) = 1 - m(h), \qquad s = 1/(1 - h). \tag{8}$$

The function $F(s)$ is analytic off the unit interval [0, 1] in the s-plane, and admits the integral representation

$$F(s) = 1 - \frac{\epsilon^*}{\epsilon_2} = \int_0^1 \frac{\mathrm{d}\mu\,(z)}{s - z}. \tag{9}$$

Here the positive measure μ on [0, 1] is the spectral measure of the self-adjoint operator $\Gamma\chi$, where $\Gamma = \nabla(-\Delta)^{-1}(\nabla\cdot)$.

The integral representation (9) is the Stieltjes transformation of the measure μ, it presents $F(s)$ as a Stieltjes function. An important feature of this representation is that it separates the properties of the mixture constituents, which are contained in the variable s, from the structural information about the geometry of the mixture, which is contained in the measure μ. We exploit this property to provide an integral representation for the effective thermal conductivity γ^*. We introduce a complex variable $s' = 1/(1 - \gamma_1/\gamma_2)$ and show that the effective properties ϵ^* and γ^* are related through the measure μ.

Proposition 1. *The effective properties ϵ^* and γ^* of the same two-component stationary random medium are related through their integral representation with the same function μ:*

$$\epsilon^*(s) = \epsilon_2 - \epsilon_2 \int_0^1 \frac{\mathrm{d}\mu\,(z)}{s - z}, \qquad s = \frac{1}{1 - \epsilon_1/\epsilon_2}, \tag{10}$$

$$\gamma^*(s') = \gamma_2 - \gamma_2 \int_0^1 \frac{\mathrm{d}\mu\,(z)}{s' - z}, \qquad s' = \frac{1}{1 - \gamma_1/\gamma_2}. \tag{11}$$

If the function μ is known from the measurements of ϵ^*, evaluation of the effective thermal conductivity γ^* reduces to a calculation of the integral in (11).

We consider first a normalized problem and outline derivation of the spectral integral representation for the effective property following [23]. Then we derive conditions for the measured values of the effective permittivity ϵ^* that allow us to uniquely recover the function μ.

3. Spectral representation for the effective property

We consider a random mixture of two materials with the values of the conductivity h in the region $\mathcal{O}_1$, and of the unit conductivity in the region $\mathcal{O}_2$. The conductivity of the medium is a random function $\sigma(x, \eta)$,

$$\sigma(x,\eta) = h\,\chi(x,\eta) + (1 - \chi(x,\eta)). \tag{12}$$

The electric and current fields, $E(x, \eta)$ and $J(x, \eta)$, satisfy (2), hence

$$\nabla \cdot (h\chi + 1 - \chi)\, E = 0. \tag{13}$$

The last expression can be brought to the form

$$\nabla \cdot\ \chi\, E = s\,\nabla \cdot\ E, \qquad s = \frac{1}{1-h}. \tag{14}$$

Let $\nabla\phi$ be a perturbation of the constant field e_k, so that $E = e_k + \nabla\phi$. Then,

$$\nabla \cdot\ \chi\,(\nabla\phi + e_k) = s\,\Delta\phi, \tag{15}$$

where $(-\Delta)$ is the Laplace operator, and

$$(\nabla\phi + e_k) + \frac{1}{s}\nabla(-\Delta)^{-1}\nabla \cdot \chi(\nabla\phi + e_k) = e_k. \tag{16}$$

Let $\Gamma = \nabla(-\Delta)^{-1}(\nabla\cdot)$, so that Γ is an operator projecting vector fields onto a subspace of curl free, zero mean fields. Then

$$E = s(sI + \Gamma\chi)^{-1} e_k. \tag{17}$$

The formula (17) represents E as a function of the operator $\Gamma\chi$. Using the spectral resolution of $\Gamma\chi$ with the projection valued measure Q, one can derive the following representation for E:

$$E(s) = \int_0^1 \frac{s}{s-z}\,\mathrm{d}Q\,(z)\,e_k. \tag{18}$$

Next we obtain the integral representation for the function $F(s)$ on the plane of the complex variable s. Consider a function $F(s)$,

$$F(s) = 1 - \sigma^*(s) = 1 - \langle (h\chi + 1 - \chi)\,E,\ e_k\rangle = \langle s^{-1}\,\chi\,E,\ e_k\rangle. \tag{19}$$

Using (18) we obtain

$$F(s) = \langle \chi\,(sI + \Gamma\,\chi)^{-1} e_k, e_k\rangle = \int_0^1 \frac{\langle \chi\,\mathrm{d}Q\,(z)\,e_k,\ e_k\rangle}{s-z}. \tag{20}$$

Introduce a function μ corresponding to the spectral measure Q, $\mathrm{d}\mu(z) = \langle \chi\,\mathrm{d}Q\,(z)e_k, e_k\rangle$. We notice that μ is a positive function of bounded variation, and measure of any subinterval $[z', z'') \subset [0, 1]$ is $\mu([z', z'')) = \mu(z'') - \mu(z')$. We have

$$F(s) = \int_0^1 \frac{\mathrm{d}\mu\,(z)}{s-z}. \tag{21}$$

Recalling that $h = \epsilon_1/\epsilon_2$, so that $s = 1/(1 - \epsilon_1/\epsilon_2)$, we find that (21) results in the representation for ϵ^* in (10).

Now, for given values γ_1, γ_2 in (4), we can introduce $s' = 1/(1 - \gamma_1/\gamma_2)$, $s' \notin [0, 1]$. The integral representation for the effective thermal conductivity γ^* is

$$\gamma^*(s') = \gamma_2(1 - F(s')) = \gamma_2\left(1 - \int_0^1 \frac{\mathrm{d}\mu\,(z)}{s'-z}\right). \tag{22}$$

As a result, the effective property γ^* can be readily evaluated if the function μ is known. We associate the measure μ with the structural function of the mixture.

Obviously, we could consider evaluation of the effective magnetic permeability, hydraulic conductivity, or diffusion coefficient, of the same medium, with an appropriate substitution of the corresponding physical fields.

4. Uniqueness of reconstruction of the spectral measure

The following theorem describes conditions when the function μ can be recovered from the measured effective property.

Uniqueness theorem. *The measure μ can be uniquely reconstructed if the function $F(s)$ is known on an open set $\mathcal{C}$ of the complex variable s with a limiting point.*

Let an analytic function $F(s)$ be given on an open set $\mathcal{C}$. It can be uniquely analytically continued on the whole domain of analyticity. The point $s = \infty$ corresponds to a homogeneous medium, $\epsilon_1 = \epsilon_2$, with $F(\infty) = 0$. The Laurent expansion of the function $F(s)$ centred at infinity is

$$F(s) = \sum_{k=1}^{\infty} \frac{c_k}{s^k}. \tag{23}$$

Using the Laurent expansion of the integral kernel, we obtain a series representation,

$$F(s) = \sum_{n=0}^{\infty} \frac{1}{s^{n+1}} \int_0^1 z^n \, \mathrm{d}\mu\,(z). \tag{24}$$

The integrals in (24) are Stieltjes moments μ_n of the measure μ:

$$\mu_n = \int_0^1 z^n \, \mathrm{d}\mu\,(z), \qquad n = 0, 1, 2, \ldots. \tag{25}$$

Comparing the series

$$F(s) = \frac{\mu_0}{s} + \frac{\mu_1}{s^2} + \frac{\mu_2}{s^3} + \cdots, \tag{26}$$

with (23), the moments $\{\mu_n\}$ of the measure μ can be determined. The problem of reconstruction of the measure μ on the unit interval from its known moments $\{\mu_n\}$ is the Hausdorff moment problem. This problem has a unique solution [1, 34].

Conditions for the moment problem to possess a unique solution when $\mu(z)$ is constant outside a given finite interval were formulated by Hausdorff. Let us introduce some notation:

$$\delta^k \mu_n = \mu_n - \binom{k}{1} \mu_{n+1} + \cdots + (-1)^k \mu_{n+k} = \int_0^1 t^n (1-t)^k \, \mathrm{d}\mu. \tag{27}$$

The two following lemmas formulate necessary and sufficient conditions for a sequence of moments μ_n to generate a measure μ [34].

Lemma 1. *A necessary and sufficient condition for the one-dimensional Hausdorff moment problem to have a solution, is that all differences $\delta^k \mu_n$ are non-negative:*

$$\delta^k \mu_n \geqslant 0, \qquad k,\ n = 0, 1, 2, \ldots. \tag{28}$$

To formulate the second condition, introduce λ_{Nn},

$$\lambda_{Nn} = \binom{N}{n} \delta^{N-n} \mu_n = \binom{N}{n} \int_0^1 t^n (1-t)^{N-n} \, \mathrm{d}\mu \tag{29}$$

and

$$M_1 = \lim_{N \to \infty} \sum_{n=0}^{N} |\lambda_{Nn}|. \tag{30}$$

Lemma 2. *A necessary and sufficient condition that the one-dimensional Hausdorff moment problem has a unique solution a function μ of bounded variation, is that $M_1 < \infty$. Furthermore,*

$$\int_0^1 |\,\mathrm{d}\mu\,(t)| = M_1. \tag{31}$$

It can be easily seen that for the sequence of moments (25) corresponding to the measure μ, these conditions are automatically satisfied. This completes the proof.

Remark. The set $\mathcal{C}$ of the theorem can be taken as an arc in the complex plane. Exploiting analytic dependence of the complex permittivity $\epsilon_1 = \epsilon_1(\omega)$ and $\epsilon_2 = \epsilon_2(\omega)$ on frequency ω we conclude that measurements of $\epsilon^*(\omega)$ in an interval of frequency $\omega \in (\omega_1,\ \omega_2)$ provide the required values of the function $F(s)$.

5. S-equivalence of structures

One can uniquely recover the measure μ and reconstruct information about the microstructure of the mixture from the measurements of the complex permittivity ϵ^* in a continuous interval of frequency ω and the values of the permittivity of the pure materials. However, the function μ does not necessarily uniquely determine the structure of the material. Therefore we introduce a new concept of S-equivalence of structures, reflecting classes of microstructures equivalent from the point of view of the spectral measure.

Definition. *Given two structures with the effective properties ϵ^{*_1} and ϵ^{*_2} and the permittivity of the pure materials ϵ_1 and ϵ_2 we define their microstructures as S-different, if there exist a pair of materials with the properties $\tilde{\epsilon_j} \in \mathbb{C}$, $j = 1,\ 2$, such that $\epsilon^{*_1}(\tilde{\epsilon_1}, \tilde{\epsilon_2}) \neq \epsilon^{*_2}(\tilde{\epsilon_1}, \tilde{\epsilon_2})$. Otherwise, these two structures are S-equivalent.*

On the s-plane, the S-equivalence of the two structures means that the corresponding functions $F^i(s)$, $i = 1, 2$, coincide $\forall s \in \mathbb{C}$. Applying the uniqueness theorem, we conclude that S-equivalent structures correspond to the same spectral function μ. In contrast, for S-different structures, there exists a point $\tilde{s} \in \mathbb{C}$ such that $F^1(\tilde{s}) \neq F^2(\tilde{s})$. Using the analyticity of the functions F^i we conclude that the S-different structures correspond to different spectral functions μ. The inverse homogenization approach is based on recovering the spectral measure μ associated with the geometric structural function. It allows us to distinguish S-different microstructures, but it is not sensitive to the S-equivalent geometries. It then follows that S-equivalent structures have the same effective properties for any initial materials filling in the geometric structure. The next proposition results as a corollary from the uniqueness theorem.

Proposition 2. *If the function $F(s)$ is known on an open set $\mathcal{C}$ in the complex s-plane, the geometries of different mixtures are distinguishable by the effective measurements up to the introduced S-equivalence of the structures.*

In order to recover geometrical information from the measurements of the effective complex permittivity, we can reconstruct the measure μ which generates measured values ϵ^*. Comparison of the expansion of $F(s)$ (26) with a similar expansion of a resolvent representation for $F(s)$ [23] yields

$$\mu_n = (-1)^n \langle \chi(\Gamma\chi)^n e_k, e_k \rangle. \tag{32}$$

If p_1 and $p_2 = 1 - p_1$ are the volume fractions of the components in the mixture, then $\mu_0 = p_1$, and if the material is statistically isotropic, $\mu_1 = p_1 p_2 / d$ where d is dimension. In general, the known $(n+1)$-point correlation function of the medium allows calculation of μ_n [23]. The integral representation (9) was used to produce bounds on ϵ^*, or $F(s)$, obtained by fixing s in (9), varying over admissible measures μ (or admissible geometries), such as those that satisfy only $\mu_0 = p_1$, and finding the corresponding range of values of $F(s)$ in the complex plane [6, 12, 23, 29, 30].

In [15], when only several data points were available, we described a set of measures consistent with the measurements:

$$\mathcal{M} = \{\mu : F_\mu(s) = 1 - \epsilon^*/\epsilon_2\}. \tag{33}$$

In that case, we could not determine the moments, nor the structure of the material. Indeed, there exist a great variety of microstructures generating the same response under the applied field. Instead, we could determine an interval confining the first moment of the measure μ, which provides an interval of uncertainty for the volume fraction of one material in the mixture. When several measurements corresponding to the same structure of material are available, such as for example, measurements for several different frequencies, the bounds for the volume fraction are given by an intersection of all admissible intervals [14, 15, 28, 36]. The uniqueness theorem establishes the requirements for the measurements needed to uniquely reconstruct the spectral measure μ. The set $\mathcal{M}$ is reduced in this case to one point. The moments μ_n (25) of this function μ contain geometric information about the structure. Different microgeometries corresponding to the same sequence $\mu_0, \mu_1, \ldots$ are the S-equivalent structures that are not distinguishable by homogenized measurements.

6. Reduction to the inverse potential problem

Here we demonstrate that the problem of reconstruction of the spectral measure μ can be regarded as inverse potential problem. Let $K(\zeta, z)$ be a fundamental solution of the Laplace operator, $(-\Delta)$, in R^2,

$$K(\zeta, z) = \frac{-1}{2\pi} \ln |\zeta - z|, \tag{34}$$

and let the potential $U(\cdot\,; \mu)$ of a measure μ be

$$U(\cdot\,; \mu) = \int K(\zeta, z)\, \mathrm{d}\mu\,(z). \tag{35}$$

The potential problem with a real-valued measure can be embedded in a complex plane $\zeta = x + \mathrm{i}y$ as follows: introduce complex differentiation

$$\partial/\partial\zeta = (\partial/\partial x - \mathrm{i}\,\partial/\partial y)/2, \qquad \partial/\partial\bar{\zeta} = (\partial/\partial x + \mathrm{i}\,\partial/\partial y)/2 \tag{36}$$

and consider a complex potential of the measure μ:

$$U_\zeta\,(\cdot\,; \mu) = \frac{-1}{4\pi} \int \frac{\mathrm{d}\mu\,(z)}{\zeta - z} = \frac{-1}{2\pi} \frac{\partial}{\partial\zeta} \int \ln |\zeta - z|\, \mathrm{d}\mu\,(z). \tag{37}$$

It can be shown that the logarithmic and complex potentials of a real-valued measure are equivalent (see [25]).

Proposition 3. *Function $F(s)$ in (9) admits a representation*

$$F(s) = \frac{\partial}{\partial s} \int \ln |s - z|\, \mathrm{d}\mu\,(z), \qquad \partial/\partial s = (\partial/\partial x - \mathrm{i}\,\partial/\partial y). \tag{38}$$

Indeed, if real-valued measures μ_1 and μ_2 are supported on [0, 1], and their logarithmic potentials are equal outside a region containing the unit interval, the equality of their complex potentials follows from (37). On the other hand, for a real-valued measure μ with a compact support, the logarithmic potential U is also real-valued. Hence, if $F(s) = 0$ outside a region containing the support of μ then $\partial U/\partial s = 0$ and $\partial U/\partial x = \partial U/\partial y = 0$. Hence the potential U is constant, and from asymptotic behaviour at infinity follows that the constant is zero.

We notice that the Stieltjes integral representation is a key representation in a remarkable connection between Pade approximants, orthogonal polynomials and continued fractions (see an extensive monograph [3] on this subject). Various numerical procedures based on these different approaches can be developed for solution of the problem. However, as we will see in the next section, the problem is ill-posed and requires regularization to develop a stable numerical algorithm.

The problem of reconstruction of the measure μ is equivalent to the inverse potential problem. The potential function u is a solution to the Poisson equation

$$-\Delta u = \psi, \qquad \mathrm{supp}(\psi) \subset \Omega, \tag{39}$$

where ψ is the density of the mass distribution in Ω. The solution of the problem is given by the Newtonian potential (35) with $\mathrm{d}\mu(z) = \psi\,\mathrm{d}z$, $z \in \Omega$. The forward problem is to find u outside Ω given ψ. The problem is well posed: its solution exists for any integrable ψ, and for a distribution, and unique and stable with respect to standard functional spaces. Usually, measured data of the normal derivative or the gradient of the potential u are available on a part of the boundary $\partial\Omega$ of the domain Ω. The inverse problem is to find ψ given values of $\partial u/\partial n$, or ∇u. Generally, the solution of this problem is non-unique. However, it is possible to show uniqueness for special kinds of density ψ, such as for a harmonic function or a characteristic function of an unknown star-shaped domain. The main feature of this inverse problem is its ill-posedness, that manifests itself in many computational difficulties.

7. Regularized problem

We consider (38). Let A be an operator mapping the set of measures $\mathcal{M}[0, 1]$ on the unit interval onto the set of complex potentials defined on a curve $\mathcal{C}$: $\zeta(s) = 0$:

$$A\mu(s) = f(s) + \mathrm{i}g(s) = \frac{\partial}{\partial s}\int_0^1 \ln|s - z|\,\mathrm{d}\mu(z), \qquad s \in \mathcal{C}. \tag{40}$$

When the curve $\mathcal{C}$ does not intersect the unit interval of the real axis, the kernel of the operator A is continuous on $\mathcal{M} \times L^2(\mathcal{C})$. Hence the operator A is a completely continuous operator. The inverse operator A^{-1} in this case is not bounded, and the inverse problem is ill-posed. Practically, this means that small variations in the data or computational noise in a numerical algorithm can lead to arbitrary large variations of the solution. This ill-posedness of the problem is well known in the inverse potential theory. It makes it impossible to improve resolution by increasing the accuracy of the measurements without regularization.

To construct the solution we formulate the minimization problem:

$$\|A\mu - F\| \to \min_{\mu\in\mathcal{M}}, \tag{41}$$

where $\|\cdot\|$ is the $L^2(\mathcal{C})$-norm, F is the function of the measured data, $F(s) = 1 - \epsilon^*(s)/\epsilon_2$, $s \in \mathcal{C}$. The solution of the problem does not continuously depend on the data, and the problem requires a regularization technique. The measurements are of limited precision, therefore only a perturbed function F^δ is available. In addition, an upper error bound δ for the noise level is usually known, $\|F - F^\delta\| \leqslant \delta$. Consider a set $\mathcal{M}_\delta$ of functions μ satisfying the measured data within the δ-error

$$\mathcal{M}_\delta = \left\{\mu \in \mathcal{M} : \|A\mu - F^\delta\| \leqslant \delta\right\}. \tag{42}$$

Unboundness of the operator A^{-1} implies that the set (42) is unbounded, which leads to arbitrary large variations in the solution.

In order to construct a regularization algorithm we introduce a stabilization functional $J(\mu)$ which constrains the set of minimizers. As a result, the solution depends continuously on the input data. Instead of minimizing (41) over all functions in $\mathcal{M}$, we seek to minimize it over a convex subset of functions which satisfy $J(\mu) \leqslant \beta$, for some scalar $\beta > 0$. A particular choice of J significantly determines the solution. Since the solution of the constrained minimization problem

$$\min_{\mu:\ J(\mu)\leqslant\beta} \|A\mu - F^\delta\| \tag{43}$$

occurs on the boundary of the constrained region (see, for instance, [8]) where $J(\mu) = \beta$, we can reformulate (43) in terms of an unconstrained minimization problem using the Lagrange multipliers method. This approach leads to an equivalent formulation that uses the Tikhonov regularization functional $\mathcal{J}^\alpha(\mu, F^\delta)$, so that the problem (43) is equivalent to solving the unconstrained minimization problem with a regularization parameter α (see [11, 35]):

$$\mathcal{J}^\alpha\left(\mu, F^\delta\right) = \|A\mu - F^\delta\|^2 + \alpha J(\mu), \qquad \mathcal{J}^\alpha\left(\mu, F^\delta\right) \to \min_{\mu\in\mathcal{M}}. \tag{44}$$

8. Quadratic penalization

Different types of stabilization functionals generate different solutions. In the case of a quadratic stabilization functional, such as norm or semi-norm of the solution (or a quadratic functional of the solution), the minimization problem becomes

$$\min_{\mu\in\mathcal{M}} \left\{\left\|A\mu - F^\delta\right\|_2^2 + \alpha\,\|L\mu\|_H^2\right\}, \tag{45}$$

where H is an appropriate space of functions and L is a chosen linear operator.

The advantage of using a quadratic stabilization functional is a linearity of the corresponding Euler equation resulting in efficiency of the numerical schemes:

$$\mu_\alpha = \left(A^*A + \alpha L^*L\right)^{-1} A^*F^\delta. \tag{46}$$

The reconstructed solution necessarily possesses a certain smoothness. We illustrate this smoothing effect using as an example the regularization scheme with the L^2-norm stabilization functional. Consider singular value decomposition of the operator A with a singular system $(\lambda_n, \psi_n, \phi_n)$: $A\phi_n = \lambda_n\psi_n$, $A^*\psi_n = \lambda_n\phi_n$ for all $n = 1, 2, \ldots$.

Figure 1 shows the first few singular values of the discretized operator A computed for the numerical example below. Only the first two of the singular values are significantly different from zero. It is obvious that the inversion of this operator cannot be performed numerically without developing a regularized computational scheme.

Using the quadratic penalization approach with $L = I$, the unique solution (46) of the minimization problem can be written in the form

$$\mu_\alpha = \sum_{n=1}^{\infty} \frac{\lambda_n}{\lambda_n^2 + \alpha}\,(F^\delta, \psi_n)\,\phi_n. \tag{47}$$

The smallest eigenvalue of $A^*A + \alpha I$ is larger than α, and the operator is continuously invertible. On the other hand, the damping effect of the regularization parameter shows itself in strong

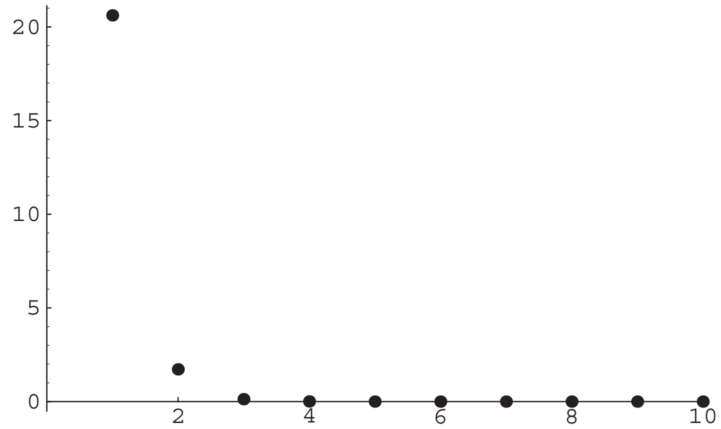

Figure 1. The first ten singular values of the operator A.

attenuation of the components of the solution corresponding to high-frequency oscillating eigenfunctions ψ_n. Indeed, for $\alpha \ll \lambda_n$,

$$\frac{\lambda_n}{\lambda_n^2 + \alpha} \approx \frac{1}{\lambda_n}, \tag{48}$$

the regularizing effect does not appear in the corresponding components of the solution. But for $\alpha \gg \lambda_n$,

$$\frac{\lambda_n}{\lambda_n^2 + \alpha} \approx \frac{\lambda_n}{\alpha} \ll \lambda_n, \tag{49}$$

and the high-frequency components are eliminated. This results in stability of the reconstructed solution, containing however, only a smooth counterpart.

9. Total variation regularization

Since the function μ is a function of bounded variation, we consider an alternative nonquadratic stabilization functional that imposes constraint on the variation of the solution in the domain. The total variation functional $J_{\mathrm{tv}}(\mu)$ is the variation of the function μ:

$$J_{\mathrm{tv}}(\mu) = \int_0^1 |\,\mathrm{d}\mu\,(z)|. \tag{50}$$

The constrained least square minimization with the total variation functional was successfully used in image reconstruction and denoising problems [13, 37] as well as in the inverse conductivity problem [19], and inverse potential problem in [10] and in the pioneering work of Sabatier [33], studying properties of the solution stemming from the non-negativity constraint. It was noticed that the total variation penalization does not impose smoothness on the solution which permits recovering blocky and contrast structures.

For an absolutely continuous function μ with the derivative $\psi(z)$, corresponding to the mass density in the potential problem,

$$J_{\mathrm{tv}}(\mu) = \int_0^1 |\mu'(z)|\,\mathrm{d}z = \int_0^1 |\psi(z)|\,\mathrm{d}z. \tag{51}$$

A constraint for the variation of the function ψ is used in image reconstruction and inversion algorithms:

$$J_{\mathrm{tv}}(\psi) = \int_0^1 |\psi'(z)|\,\mathrm{d}z. \tag{52}$$

Since $\|\psi\|_{L_1} \leqslant \|\partial\psi/\partial x\|_{L_1}$ [22], the penalization based on (52) taken as the stabilizing functional also constrains the variation of μ. In the next section we show results of numerical simulation using total variation constraint as a stabilizing condition in the problem of reconstruction of the measure μ. The gradient of the J_{tv} functional is calculated using a scheme developed in [19].

10. Discretization problem

We discretize the problem to construct a numerical scheme. Let the unit interval [0, 1] be partitioned into subintervals $[x_{i-1},\ x_i)$ of the length Δx. We approximate the function $\mathrm{d}\mu\,(z)$ by a linear combination of point masses δ_{z_i} concentrated in the central point z_i of each subinterval as follows:

$$\mathrm{d}\mu = \sum_i \mu^i\,\delta_{z_i}, \qquad \mu^i = \mu([x_{i-1},\ x_i)) = \mu(x_i) - \mu(x_{i-1}). \tag{53}$$

For an absolutely continuous function μ, with $\mathrm{d}\mu = \psi\,\mathrm{d}x$,

$$\mu^i = \int_{x_{i-1}}^{x_i} \psi(x)\,\mathrm{d}x = \psi_i\,\Delta x, \tag{54}$$

where ψ_i is the mean value of ψ on the ith subinterval.

The value of $(A\mu)(s)$ at the points s on the curve $\mathcal{C}$ is

$$(A\mu)(s) = \frac{\partial}{\partial s}\sum_i \ln|s - z_i|\,\mu^i, \qquad s \in \mathcal{C}. \tag{55}$$

We can discretize the problem keeping the same notation F for the vector of data measured at points $s_1, s_2, \ldots, s_N$ on the curve $\mathcal{C}$:

$$\|Km - F\|^2 + \alpha J\,(m) \to \min_{m \in R^n}, \tag{56}$$

where we introduce a vector $m = (\mu^1, \mu^2, \ldots, \mu^n)^T$ and $K = \{a_{ki}\}$ is a matrix with complex entries

$$a_{ki} = \frac{\partial}{\partial s}\ln|s - z_i|\bigg|_{s=s_k}, \qquad s_k \in \mathcal{C}. \tag{57}$$

11. Numerical example

To demonstrate the developed technique we consider a numerical example simulating properties of a two-component mixture of known simple geometry. We assume that the mixture is a dilute periodic composite, consisting of ellipsoids of volume v with the complex permittivity ϵ_1 embedded in a much larger homogeneous host of the permittivity ϵ_2. The effective complex permittivity of such a medium is calculated as

$$\epsilon^* = \epsilon_2 + \epsilon_2 \frac{v}{V}\frac{\epsilon_1 - \epsilon_2}{\epsilon_2 + n(\epsilon_1 - \epsilon_2)} \tag{58}$$

where V is the total volume, and n is depolarization factor. It can be easily seen that ϵ^* diverges when

$$\epsilon_1 = -(1 - n)\epsilon_2/n. \tag{59}$$

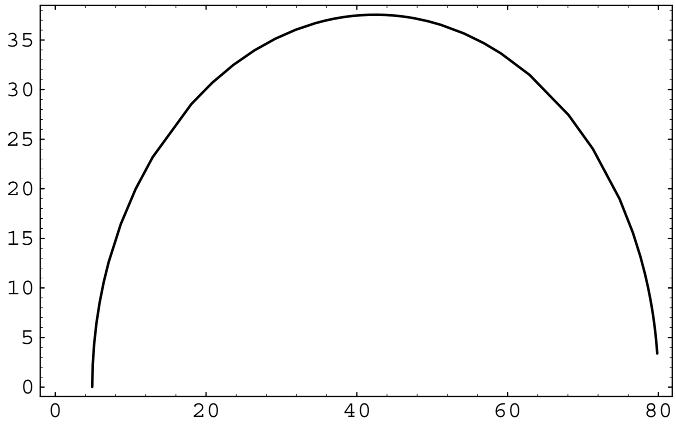

Figure 2. Water dispersion curve.

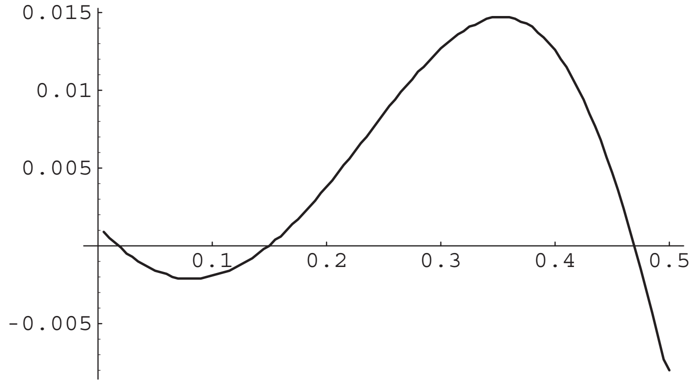

Figure 3. Reconstruction of a point mass $0.5\,\delta_{1/3}$ concentrated at $z = 1/3$. The numerical algorithm is based on the l^2-norm stabilization functional introduced to constrain the set of solutions.

This gives a pole at $h_0 = -(1-n)/n$ or transforming to the s-plane, the pole at $z_0 = 1/(1-h) = n$. We consider a case when the embedded particles are of spherical shape, in this case $n = 1/3$. Hence the measure μ corresponds to the point mass concentrated at $z_0 = 1/3$.

We also assume that one of the components is water, the permittivity of water depends on frequency. Let this dependence be described by the Debye relaxation function

$$\epsilon = \epsilon_\infty + \frac{\epsilon_s - \epsilon_\infty}{1 + i\omega\tau}. \tag{60}$$

Here ϵ_s is the static dielectric constant (the value at zero frequency), ϵ_∞ is the value at high frequency, $\omega = 2\pi f$ is the angular frequency, with f representing the frequency of the field, and τ the relaxation time. In the present numerical example these parameters have the values $\epsilon_s = 80$, $\epsilon_\infty = 4.9$, $\tau = 7.20$ ps. Figure 2 shows the water dispersion curve. The second component in the mixture is assumed to have complex permittivity of sandstone, which does not vary with frequency.

We calculate the effective complex permittivity of the mixture with this simple geometry for a number of sampling points in a specified range of frequency and use the imaginary part as data points for the inversion procedure.

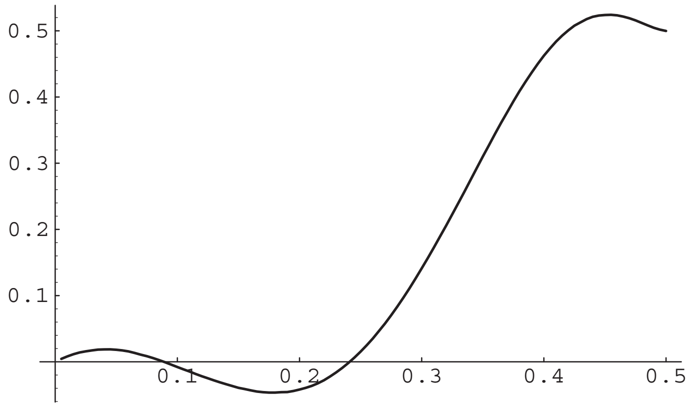

Figure 4. The results of reconstruction of $\mu(z)$ using the algorithm with a quadratic stabilization functional constraining the l^2-norm of the solution. The true solution is a step function $0.5\ H(z-1/3)$.

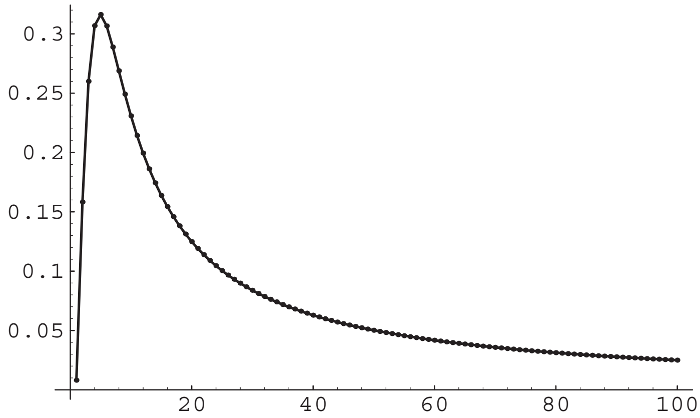

Figure 5. Imaginary part of the function F. Calculated values are represented by dots, the curve indicates the measured data.

Figure 3 shows the results of reconstruction of a point mass $0.5\ \delta_{1/3}$ concentrated at $z = 1/3$ using the algorithm with quadratic stabilization functional constraining the l^2-norm of the solution. The corresponding function $\mu(z)$ is shown in figure 4. The true solution is a step function $0.5\ H(z - 1/3)$. One can see that the reconstructed solution is reminiscent of the true step function, however, it is much smoother.

Figure 5 shows a good agreement between the measured values of the imaginary part of the function F and the values computed using the reconstructed measure μ. Here the calculated values are shown by dots, the curve indicates the measured data. Such a good agreement even in the quadratic stabilization case, is readily explained by the smoothing properties of the operator A. This indicates that the reconstructed function μ can be successfully used for evaluation of other effective properties, as well as computation of the real part of ϵ^* from the measured imaginary part based on Kramers–Kronig's relations [20, 26].

However, in a number of interesting applications, such as percolation and estimation of the hydraulic conductivity of a porous medium, the initial materials' constants are in the vicinity of the spectral interval. In this case, special care should be taken to ensure accurate

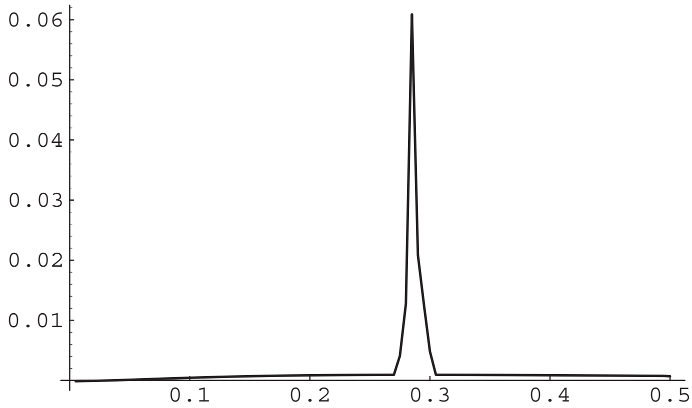

Figure 6. Reconstruction of the measure μ using the total variation stabilization functional. The true solution is a point mass $0.1\,\delta_{1/3}$.

reconstruction of the function μ. To pursue this, we developed a numerical scheme based on a total variation stabilization functional. In this numerical simulation the true solution is a point mass $0.1\,\delta_{1/3}$. The reconstruction of this delta function solution using the total variation stabilization functional is shown in figure 6.

12. Conclusion

The geometric structural function associated with the spectral measure μ in the Stieljes representation of the effective complex permittivity of a mixture is uniquely recovered provided the effective permittivity measurements are available in a continuous range of frequency of the applied field. This geometric structural function contains information about the microstructure of a mixture. We introduce S-equivalence of the geometric structures corresponding to the same spectral measure μ, and show that the microstructures of different mixtures can be identified up to the introduced equivalence. The reconstructed spectral measure μ is used to calculate other effective properties of the same mixture.

Acknowledgments

The author is grateful to Kenneth Golden and Graeme Milton for many helpful discussions and comments on different parts of this work. The work was supported by ONR grant no N000149310141.

References

[1] Akhiezer N I 1965 *The Classical Moment Problem* (New York: Hafner Publishing Company)
[2] Anger G 1990 *Inverse Problems in Differential Equations* (New York: Plenum)
[3] Baker G A Jr and Graves-Morris P 1996 *Pade Approximants* 2nd edn (Cambridge: Cambridge University Press)
[4] Bergman D J 1978 The dielectric constant of a composite material—A problem in classical physics *Phys. Rep.* C **43** 377–407
[5] Bergman D J 1980 Exactly solvable microscopic geometries and rigorous bounds for the complex dielectric constant of a two-component composite material *Phys. Rev. Lett.* **44** 1285
[6] Bergman D J 1982 Rigorous bounds for the dielectric constant of a two-component composite *Ann. Phys., NY* **138** 78

[7] Bergman D J 1993 Hierarchies of Stieltjes functions and their application to the calculation of bounds for the dielectric constant of a two-component composite medium *SIAM J. Appl. Math.* **53** 915–30

[8] Bertero M 1986 Regularization methods for linear inverse problems *Inverse Problems, Montecatini Terme* ed G Talenti (Berlin: Springer) pp 52–112

[9] Berryman J G and Blair S C 1987 Kozeny–Carman relations and image processing methods for estimating Darcy's constant *J. Appl. Phys.* **62** 2221–8

[10] Bertete-Aguirre H, Cherkaev E and Oristaglio M Non-smooth gravity problem with total variation penalization functional *Geophys. J. Int.*

[11] Björck A 1996 *Numerical Methods for Least Squares Problems* (Philadelphia: SIAM)

[12] Bruno O P 1991 Taylor expansions and bounds for the effective conductivity and the effective elastic moduli of multicomponent composites and polycrystals *Asymptotic Anal.* **4** 339–65

[13] Chan T F, Golub G H and Mulet P 1996 A nonlinear primal-dual method for total variation-based image restoration *ICAOS'96 (Paris)* pp 241–52

[14] Cherkaeva E and Tripp A C 1996 Bounds on porosity for dielectric logging *ECMI96: 9th Conf. European Consortium for Mathematics in Industry (Denmark)* pp 304–6

[15] Cherkaeva E and Golden K M 1998 Inverse bounds for microstructural parameters of a composite media derived from complex permittivity measurements *Waves Random Media* **8** 437–50

[16] Cherkaev E, Khan A H and Tripp A C 2000 Fracture surface characterization through x-ray tomography *Proc. 25th Workshop on Geothermal Reservoir Engineering (Stanford)*

[17] Day A R and Thorpe M F 1996 The spectral function of random resistor networks *J. Phys.: Condens. Matter* **8** 4389–409

[18] Day A R, Thorpe M F, Grant A R and Sievers A J 2000 The spectral function of a composite from reflectance data *Physica* B **279** 17–20

[19] Dobson D and Santosa F 1994 An image-enhancement technique for electrical impedance *Inverse Problems* **10** 317–34

[20] Eyre D, Milton G W and Mantese J V 1997 Finite frequency range Kramers Kronig relations: Bounds on the dispersion *Phys. Rev. Lett.* **79** 3062–4

[21] Gajdardziska-Josifovska M, McPhedran R C, McKenzie D R and Collins R E 1989 Silver-magnesium fluoride cermet films. 2: Optical and electrical properties *Appl. Opt.* **28** 2744–753

[22] Giusti E 1984 *Minimal Surfaces and Functions of Bounded Variation* (Basle: Birkhauser)

[23] Golden K and Papanicolaou G 1983 Bounds on effective parameters of heterogeneous media by analytic continuation *Commun. Math. Phys.* **90** 473–91

[24] Golden K 1995 Bounds on the complex permittivity of sea ice *J. Geophys. Res. (Oceans)* **100(C7)** 699–711

[25] Isakov V 1990 *Inverse Source Problems (AMS, Mathematical Surveys and Monographs vol 34)* (Providence, RI: American Mathematical Society)

[26] Melrose D B and McPhedran R C 1991 *Electromagnetic Processes in Dispersive Media* (Cambridge: Cambridge University Press)

[27] McPhedran R C, McKenzie D R and Milton G W 1982 Extraction of structural information from measured transport properties of composites *Appl. Phys.* A **29** 19–27

[28] McPhedran R C and Milton G W 1990 Inverse transport problems for composite media *Mat. Res. Soc. Symp. Proc.* **195** 257–74

[29] Milton G W 1980 Bounds on the complex dielectric constant of a composite material *Appl. Phys. Lett.* **37** 300–2

[30] Milton G W 1981 Bounds on the complex permittivity of a two component composite material *J. Appl. Phys.* **52** 5286–93

[31] Parker R L 1994 *Geophysical Inverse Theory* (Princeton, NJ: Princeton University Press)

[32] Prager S 1969 Improved variational bounds on some bulk properties of a two-phase random medium *J. Chem. Phys.* **50** 4305–12

[33] Sabatier P C 1977 Positivity constraints in linear inverse problems I. General theory *Geophys. J. R. Astron. Soc.* **48** 415–41

Sabatier P C 1977 Positivity constraints in linear inverse problems II. Applications *Geophys. J. R. Astron. Soc.* **48** 443–59

[34] Shohat J A and Tamarkin J D 1943 *The Problem of Moments (AMS, Mathematical Surveys, No 1)* (New York: American Mathematical Society)

[35] Tikhonov A N and Arsenin V Y 1977 *Solutions of Ill-Posed Problems* (New York: Wiley)

[36] Tripp A C, Cherkaeva E and Hulen J 1998 Bounds on the complex conductivity of geophysical mixtures *Geophys. Prospect.* **46** 589–601

[37] Vogel C R and Oman M E 1996 Iterative methods for total variation denoising *SIAM J. Sci. Comput.* **17** 227–38